Available online at www.sciencedirect.com
ScienceDirect
C. R. Physique 8 (2007) 1151–1161
COMPTES RENDUS PHYSIQUE
http://france.elsevier.com/direct/COMREN/

Optical parametric sources for the infrared/Sources optiques paramétriques pour l'infrarouge

High repetition rate mid-infrared laser source

Martin Schellhorn *, Marc Eichhorn, Christelle Kieleck, Antoine Hirth

French–German Research Institute, ISL, 5, rue du General Cassagnou, 68301 Saint-Louis, France

Available online 26 October 2007

Abstract

An efficient, high-power mid-infrared laser source based on $ZnGeP_2$ (ZGP) optical parametric oscillator (OPO) is presented. Using a Q-switched Ho:YAG laser as the pump source a total output power of 10.6 W was obtained in the 3–5 μm band at 10 kHz and 8.5 W at 20 kHz. The Ho:YAG laser was pumped by two diode-pumped polarization coupled Tm:YLF lasers. Optical-to-optical efficiency achieved is >8.8% (laser-diode 792 nm to mid-IR 3–5 μm). With a commercial PtSi infrared camera (256 × 256 pixel focal plane array, 24 μm pitch) the pointing stability of Ho pump, signal and idler beam was measured to be better than 30 μrad. Whilst propagating the OPO beams over ∼100 m, little absorption for the idler beam was observed, resulting in a significant higher peak-to-peak value of ±22%, whereas the peak-to-peak stability of the signal pulses remained unchanged (±13%). ***To cite this article: M. Schellhorn et al., C. R. Physique 8 (2007).***

Résumé

Source laser à fort taux de répétition pour le mi-infrarouge. Les lasers à solide à basse énergie prennent de plus en plus d'importance dans la lutte contre les systèmes d'armes optroniques. Dans le cadre de ce contrat, un système laser dans le domaine moyen infrarouge devra être développé et jugé en termes de rendement, de qualité de faisceau, de stabilité de pointage ainsi que de comportement de propagation dans l'atmosphère.

Avec un oscillateur paramétrique optique (OPO) $ZnGeP_2$ (ZGP), pompé par un laser Ho:YAG Q-déclenché à une fréquence de 10 kHz, on a obtenu une puissance de sortie de plus de 10.6 W dans le domaine infrarouge moyen (3.9 et 4.5 μm). En revanche, le laser Ho:YAG est pompé par 2 lasers Tm:YLF couplés par polarisation et pompés par des diodes. On obtient un rendement optique-optique (longueur d'onde des diodes laser par rapport au domaine infrarouge moyen) de plus de 8.8%. La stabilité de pointage des faisceaux laser pour 2.09 μm (Ho:YAG), pour 3.9 μm (faisceau du Signal) et pour 4.5 μm (faisceau du Idler) était <30 μrad. Les mesures de propagation ont permis d'observer que la variation de l'intensité de pointe de la répartition spatiale du faisceau Idler (4.5 μm), entre les impulsions, passe d'env. ±8% à la sortie du laser à env. ±22% après une distance de 100 m. Par contre, les variations du faisceau du Signal (3.9 μm) restent inchangées à env. ±12%. Ceci s'explique par de faibles pertes par absorption du faisceau Idler, par la bande d'absorption de CO_2 à 4.25 μm ainsi que les raies de l'eau isolées ($\lambda > 4.5$ μm). ***Pour citer cet article : M. Schellhorn et al., C. R. Physique 8 (2007).***

Keywords: Tm:YLF laser; Ho:YAG laser; $ZnGeP_2$; OPO; Pointing stability

Mots-clés : Laser Tm:YLF ; Laser Ho:YAG ; $ZnGeP_2$; OPO ; Stabilité de pointage

* Corresponding author.
E-mail address: schellhorn@isl.tm.fr (M. Schellhorn).

1631-0705/$ – see front matter
doi:10.1016/j.crhy.2007.09.007

1. Introduction

Coherent radiation sources operating in the middle infrared transmission window (3 to 5 micron wavelength region) are the subject of ongoing research. Such sources are key components in directive countermeasure systems against infrared sensors. Other important applications are remote sensing, chemical/pollutants detection and Earth monitoring, to name but a few. Since there is no practical, widely tunable high-power laser source in this wavelength range, nonlinear optical conversion techniques must be used. One such configuration, called an optical parametric oscillator (OPO), can be used to convert the pump wavelength to two longer wavelengths in the infrared region. A 1 micron pump laser requires two OPO stages, because there exists at present no mature nonlinear optical material suitable for high-power operation having high transmission in the 1 and the 3 to 5 micron wavelength region. An alternative approach is to use high-power 2 micron lasers as the pump source. Although Tm^{3+} and Ho^{3+} doped laser materials have a low effective stimulated emission cross-section, they have the potential of high-energy Q-switched output under cw pumping conditions owing to their long upper-state fluorescence lifetimes ($\sim$10 ms). Tm^{3+} has high absorption peaks conveniently located for diode pumping at 0.79 μm and it exhibits cross-relaxation processes, that create two ions in the upper laser level for each pump photon absorbed. Unfortunately, Ho^{3+} has no absorption bands that coincide with the emission wavelengths for commercially available high-power diode bars. One solution to this problem is to pump the Ho:YAG laser, in-band, either extracavity with a diode-pumped Tm-doped bulk laser [1] or a cladding-pumped Tm-doped fiber laser [2], or intracavity by Tm:YAG [3] or Tm:YLF [4]. Due to the excellent beam quality of the pump sources and the very low quantum defect in the Ho:YAG, very high lasing efficiencies (80%) are attainable [5]. These Q-switched 2-μm lasers could be frequency downconverted in a ZGP based OPO, and it has been shown that over 50% conversion efficiency from 2 μm to the 3–5 μm spectral band could be achieved [6]. In the present work results from recent experiments are presented to emphasize efficiency, beam quality and pointing stability of the laser–OPO system.

2. Experimental setup

Fig. 1 shows the experimental setup of the total laser system. Two identical, polarization coupled Tm:YLF lasers were used as the pump source for the Q-switched Ho:YAG laser. The light from the Ho:YAG laser is focused to the ZGP-based OPO system that has been designed as a double-pass doubly resonant (DPDRO) OPO.

2.1. Tm:YLF laser

Each Tm:YLF laser is diode end-pumped with two fiber-coupled laser diodes (FAP-795-40C-800B, Coherent) with a fiber diameter of 800 μm and a numerical aperture of 0.12. The pump light was imaged 1:1 by use of standard optics (GLC006 and LLP113, Melles Griot). The pump beam caustic has been measured resulting in a pump spot $1/e^2$ radius of 400 μm and a divergence half angle of 85 mrad. The L-shaped cavity consists of a flat mirror (M1) with high reflectivity ($R > 99.8\%$) in the wavelength range 1.9–2.1 μm and high transmission ($T > 95\%$) at the diode-pump wavelength, a flat 45° dichroitic mirror (M2) with high reflectivity ($R > 99.9\%$) at the s-polarized component in the wavelength range 1.9–1.95 μm and high transmission at the diode-pump wavelength ($T > 98\%$), and a concave output coupler (M3) with a radius of curvature 300 mm. Using a transmission of 20% transmission of the output coupler forces oscillating of the Tm:YLF laser on several lines centered at 1910 nm. The Tm:YLF crystal dimension is 4 mm in diameter and has a 12-mm-long gain medium. The Tm dopant concentration is 3.5% at. weight. Two undoped diffusion-bonded end caps are used at both ends for an overall crystal length of 20 mm. Crystals of the Tm gain medium and the end caps are *a*-cut (crystalline '*a*' axis (σ) is along the laser rod axis, crystalline '*c*' axis (π) is along the radial rod axis). The crystal is mounted in a copper heat sink maintained at room temperature (20 °C). Both end faces of the Tm:YLF crystal are antireflection coated for wavelengths in the range 1.9–2.0 μm and high transmission ($T > 99\%$) at the diode-pump wavelength. The Tm:YLF crystal is oriented so that the *c*-axis is parallel to the plane of incidence of the 45° dichroitic mirror. A fraction of 85% of the unpolarized pump radiation is absorbed at the operating wavelength of 792 nm of the laser diodes. A 100 μm quartz etalon (Et1) was used to force oscillation of the Tm:YLF pump laser at the wavelength near the peak absorption line of Ho (1908 nm). Due to heating of the etalon the pump wavelength increased slightly from 1906.8 nm at threshold to 1908.3 nm at maximum Tm:YLF laser power. The wavelength was selected away from the water vapor lines centered at 1906.5 and 1908.5 nm, but still in

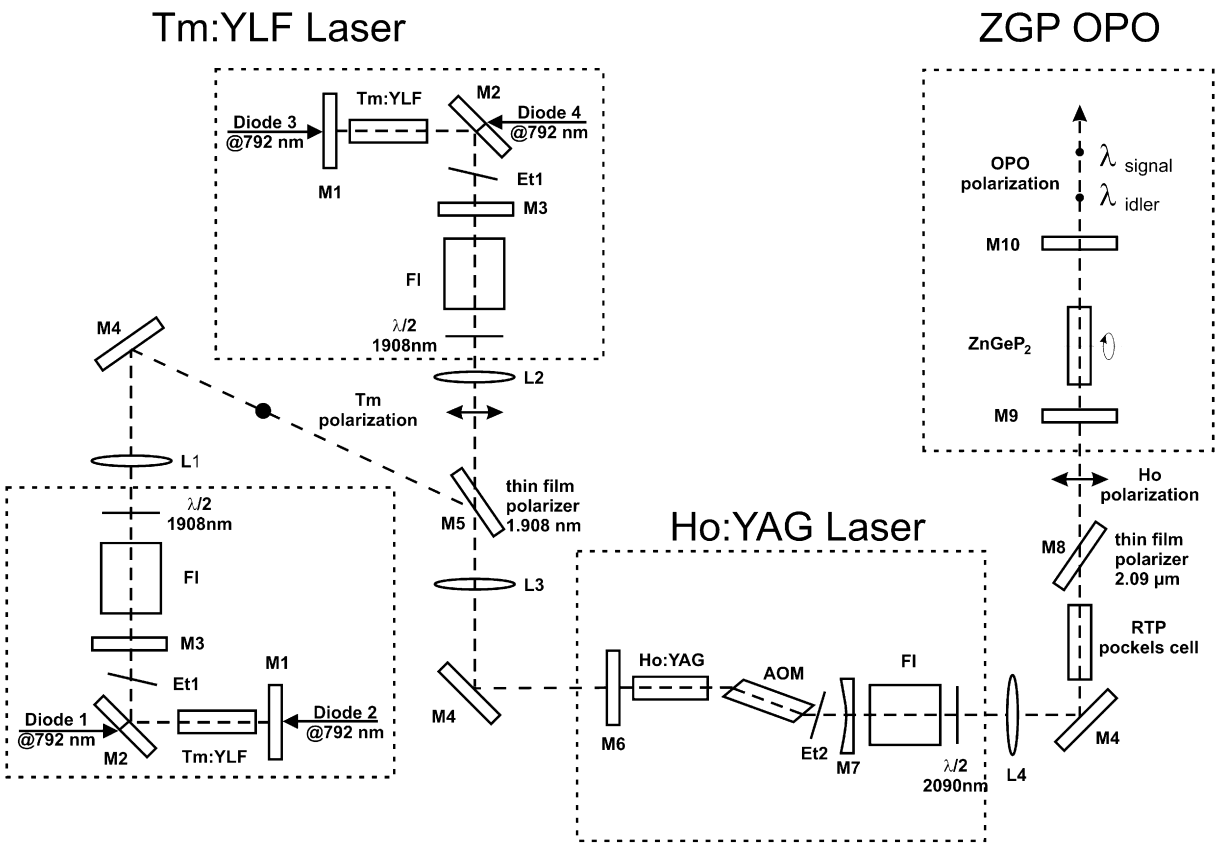

Fig. 1. Experimental setup of the total system: M1–M10, mirrors; L1–L4, lenses; $\lambda/2$, half-wave plates; Et1–Et2, etalons; FI, Faraday isolator; AOM, acusto-optic modulator. The details of the setup are described in more details in Sections 2.1–2.3.

the absorption line of Ho. Each pump beam passed through a Faraday isolator and a $\lambda/2$ plate. Each isolator consists of a Faraday rotator (I-21FR-4, Isowave) with a clear aperture of 4 mm and two thin-film polarizers, coated for the wavelength of 1908 nm. The rotation angle has been measured to be ∼54 degrees. To provide optimum isolation, the thin-film polarizers must be rotated by 36 degrees with respect to each other, resulting in a transmission of the two polarizers of ∼90%. The rotator itself transmits approximately 95%. The complete isolator's transmission is therefore ∼85%. Both Tm:YLF laser beams are collimated by lenses (L1, $f = 300$ mm; L2, $f = 250$ mm) to get approximately the same beam diameter on the thin film polarizer (M5) which has been used to couple both perpendicular polarized laser beams. Due to strong water absorption present in the 1.91-μm spectral region, the Tm lasers were enclosed in dry boxes and flushed with purged dry condensed air.

2.2. Ho:YAG laser

The Ho:YAG laser was single end-pumped by the Tm:YLF lasers. The Tm pump radiation was focused by lens L3 ($f = 250$ mm) to a $1/e^2$ diameter of 450 μm inside the Ho:YAG rod. The Ho:YAG crystal dimension is 4 mm in diameter and 28 mm in length with a holmium dopant concentration of 0.7%. Mirror M6 was flat with 98% transmission at 1.9 μm and high reflectivity ($R > 99.8\%$) at 2.1 μm. The Ho:YAG laser light is coupled out through the 60% reflective mirror M7 with a 200 mm radius of curvature. The laser was Q-switched by a fused silica acusto-optic Q-switch (QS027-10M(BR)-IS4, Gooch & Housego) with Brewster-angle end faces (crystal length 45 mm). The radio frequency (rf) was 27 MHz, and the rf power was 10 W. The pulse repetition rate was 10 kHz. Without the etalon (Et2); the laser oscillated simultaneously on 2090 and 2097 nm, which is not desired for pumping an OPO. A 100 μm quartz etalon was inserted into the resonator to force oscillation of the Ho:YAG laser at the wavelength of 2090 nm. A Faraday rotator (I-21FR-4, Isowave) with a clear aperture of 4 mm and two thin-film polarizers, coated

Table 1
List of ZGP crystal dimension, cut angle and supplier

	Dimension (mm)	Cut angle (degree)	Supplier
Crystal 1	$4 \times 4 \times 16$	52°	Inrad
Crystal 2	$5 \times 5 \times 16$	52°	Inrad
Crystal 3	$6 \times 6 \times 16$	54°	Eksma
Crystal 4	$5 \times 5 \times 18$	51°	Eksma

for the wavelength of 2090 nm was used to avoid feedback from the OPO to the Ho:YAG laser. At the Ho wavelength the rotating angle has been measured to be ∼44 degrees. The complete isolator's transmission is therefore ∼95%.

2.3. $ZnGeP_2$ optical parametric oscillator

The output from the Ho:YAG laser was focused with lens L4 ($f = 250$ mm) to a $1/e^2$ diameter waist of 750 μm inside the ZGP crystal. The Ho laser radiation passed a RTP Pockels cell and a thin film polarizer, coated for 2.09 μm. With this setup the repetition rate of the Ho:YAG pump laser could be reduced for the pointing measurements which will be described later. Four different ZGP crystals from two different suppliers have been tested. The crystals were cut for type 1 phase matching for 3–5 μm generation and antireflection (AR) coated for this wavelength range and the pump at 2090 nm. The physical dimension, cut angle and the supplier of the crystals is listed in Table 1. The resonator consisted of two flat mirrors. M9 was a CaF_2 substrate, coated for high-reflection (HR) with $R > 95\%$ for 3.9–4.6 μm and high transmission ($T \sim 94\%$) at the pump wavelength of 2090 nm. The output coupler M10 was a 2 mm thick YAG substrate, coated for high-reflection ($R > 99.7\%$) at the pump wavelength and approximately 80–90% transmission for 3–5 μm. The OPO is thus doubly resonant and double-pass pumped, and the reflection range of the HR mirror limits the tuning range of the OPO.

3. Laser results

3.1. Tm:YLF laser

The output power of the two polarization coupled Tm:YLF lasers (measured behind mirror M5) as a function of the pump diode power incident on the Tm:YLF crystals is shown in Fig. 2. A maximum laser power of 41.7 W was obtained at a pump power level of 121 W. This corresponds to a slope efficiency of 40% and an optical-to-optical efficiency of 34.5%. Taking into account the losses of the Faraday isolators of ∼15% the slope efficiency of the

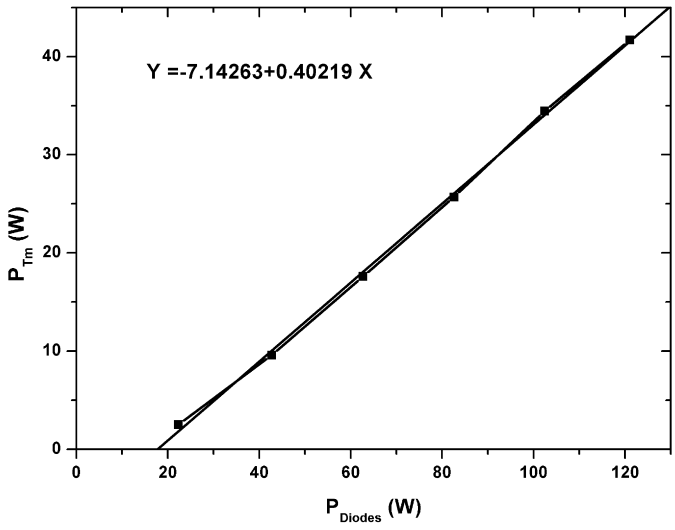

Fig. 2. Output power at 1.908 μm of the polarization coupled Tm:YLF lasers as a function of the diode power incident on the crystals.

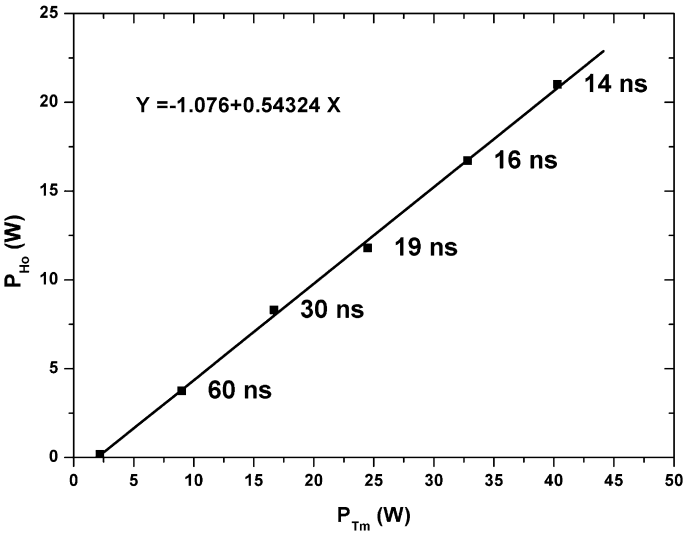

Fig. 3. Output power at 2.09 μm and pulse length (FWHM) of the Q-switched Ho:YAG as a function of Tm pump power at a repetition rate of 10 kHz.

Tm:YLF laser itself is ∼47%. The beam quality factor was measured at the maximum power output, resulting in a value of $M^2 \sim 2$. It must be pointed out that the Tm:YLF laser must be protected with an optical isolator from feedback. Even the smallest feedback results in strong power fluctuations which could damage the coatings of the crystal or mirror M2.

3.2. Ho:YAG laser

The average output power and pulse length of the Q-switched Ho:YAG laser (measured behind mirror M7) at a repetition rate of 10 kHz as a function of the Tm pump power incident on M6 is shown in Fig. 3. The output power did not change significantly between cw (with an open Q-switch) and Q-switched operation (10–50 kHz). The laser power is 21 W when 40.3 W is incident on M6. The slope efficiency is 54%, and the pump threshold is 1.9 W. The temporal pulse shape was reasonably symmetrical with a 14 ns FWHM pulse length at 10 kHz at maximum pump power. The pulse length increased nearly linear with the pulse repetition rate, as is shown in Fig. 4. The beam quality factor was measured at the maximum power output, resulting in a value of $M^2 \sim 1.1$.

3.3. $ZnGeP_2$ optical parametric oscillator

The performance of the different ZGP crystals, listed in Table 1, were tested at Ho pump power level up to 9 W. The 3–5 μm average output power as a function of launched Ho pump power on M9 at a repetition rate of 10 kHz is shown in Fig. 5. Each crystal was tilted for maximum OPO laser power. The power performance of the different ZGP crystals did not change significantly. The maximum laser power was obtained when the crystals were tuned to 3.9 μm + 4.6 μm. Note that the measured curves were taken by adjusting the pump diode laser power. Therefore, the pump pulse length is longer at low pump powers. The conversion efficiency of the OPO is ∼50%, and the slope efficiency and threshold is 90% and ∼3.5 W (350 μJ), respectively.

The OPO laser power and the beam quality of the signal beam ware measured as a function of the cavity length using crystal 1. The results are shown in Fig. 6. There is a small decrease in OPO laser power with increasing cavity length. The group of FFI (Norway) has previously shown that the output from a doubly resonant OPO pumped by a multimode beam can be significantly increased if the optical paths in the pump laser and the OPO are matched [7]. This effect is shown in Fig. 6 when the OPO resonator was adjusted to match that of the Ho:YAG laser ($x = 60$ mm), which had an optical round-trip length of 230 mm (an AOM with a length of 28 mm has been used in this experiment). The beam quality is improved from $M^2 \sim 4$ using a short resonator length to $M^2 \sim 2$ at this resonance.

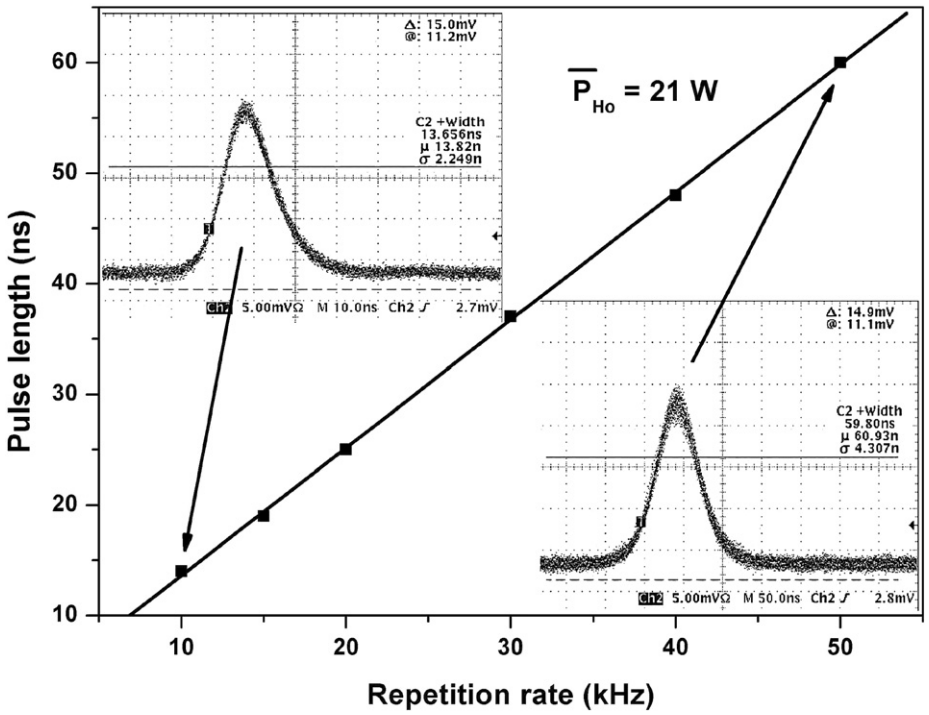

Fig. 4. Pulse length (FWHM) as a function of repetition rate at maximum laser power of 21 W. The insets show pulse shapes at 10 and 50 kHz, respectively (persistence: 500 ms).

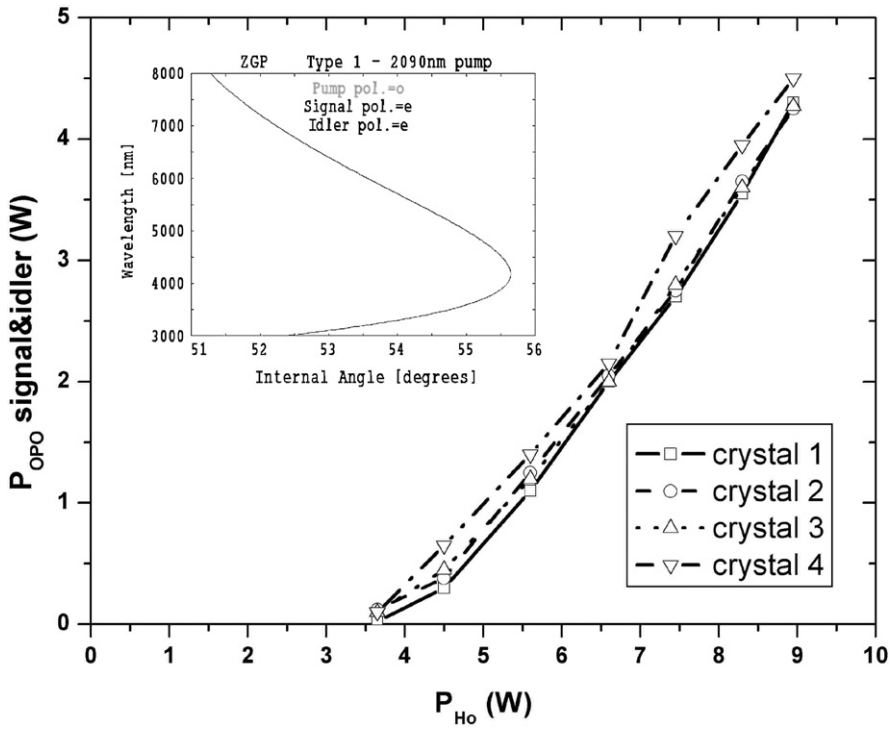

Fig. 5. 3–5 μm average output power of the ZGP OPO as a function of launched Ho pump power on M9 at a repetition rate of 10 kHz for the different ZGP crystals listed in Table 1.

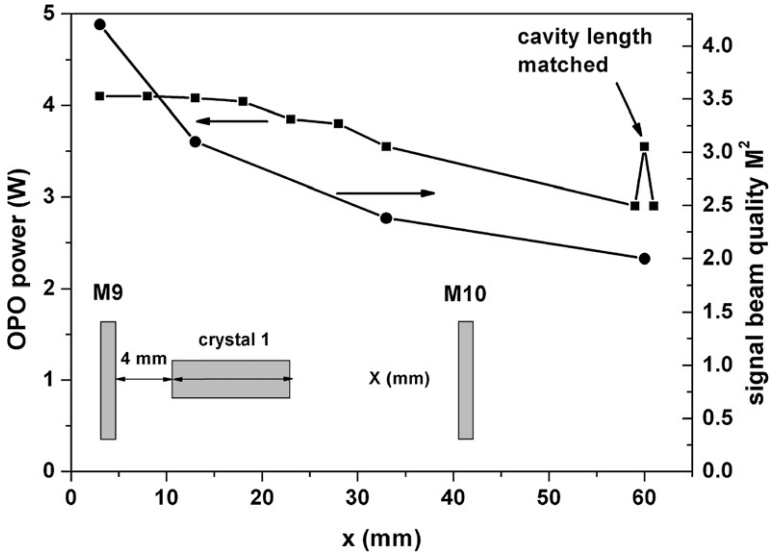

Fig. 6. OPO power and signal beam quality as a function of the distance between the ZGP crystal and output coupler M10. ZGP crystal 1 was pumped at 8.5 W at a repetition rate of 10 kHz.

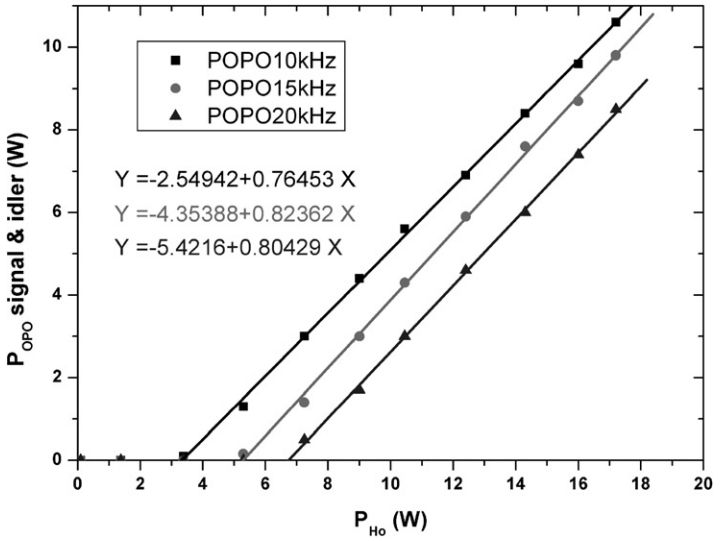

Fig. 7. The total 3–5 μm average output power of the ZGP OPO using crystal 1 as a function of launched Ho pump power on M9 at a repetition rate of 10, 15 and 20 kHz.

The ZGP OPO with crystal 1 was pumped with the maximum available Ho:YAG pump power. The 3–5 μm average output power as a function of launched Ho pump power on M9 at repetition rates of 10, 15 and 20 kHz is shown in Fig. 7. The physical resonator length was 22 mm. The total output power (signal + idler) was 10.6 W at 10 kHz, 9.8 W at 15 kHz and 8.5 W at 20 kHZ, when the OPO was pumped at 17.2 of Ho average power. This corresponds to a conversion efficiency of the OPO of 61.6%, 57% and 48.6%, when the OPO is pumped with 10, 15 and 20 kHz, respectively. Linear fits to the measured data result in slope efficiencies of 76.5%, 82.4% and 80.4% and thresholds of 3.3 W (330 μJ), 5.3 W (350 μJ) and 6.7 W (340 μJ), when the OPO is pumped with 10, 15 and 20 kHz, respectively.

4. Pointing stability

4.1. Experimental setup

The measurements of the pointing stability of the Ho:YAG laser and the ZGP OPO has been made using the European norm (EN ISO 11670) [8]. The experimental setup is shown in Fig. 8. The transmitter–telescope was formed by two spherical CaF_2 lenses ($f_1 \sim -100$ mm, $f_2 \sim 500$ mm). The telescope was adjusted in such a way that the beam diameter behind the telescope remained nearly unchanged over a propagation length of 100 m. At the OPO power level of 4 W and $M^2 \sim 4$ the beam diameter was approximately 60 mm. The receiver telescope was adjusted to a focal length of approximately 1.7 m. A PtSi infrared camera (PtSi 256 SM, Thermosensorik) with a focal plane array of 256×256 pixels (24 μm pitch) was used together with a Spriricon frame grabber to measure the beam parameters. The camera was operated in the 'rolling frame modus' at 50 Hz with an exposure time of 10 ms. To detect a single pulse the repetition rate of the Ho:YAG laser (10 kHz) was divided by a factor of 100. After 99 pulses the $\lambda/2$ voltage was applied to the RTP cell, switching the polarization of the Ho:YAG pulse from s- to p-polarization and therefore transmitted the thin film polarizer M8 and pumped the OPO. Note that the thermal load of the ZGP crystal is not the same in these measurements. In an early experiment, when we did not use M8 and the OPO was pumped with 99 s-polarized pulses (no phase matching), bulk damage in the ZGP crystal was observed, even at a low average pump power of 7 W. For the pointing measurements the receiver telescope is mounted directly behind the transmitter telescope, resulting in distance of 1.5 m between camera position and output coupler.

4.2. Experimental results

The measured positions of the centroid of the Ho:YAG, signal and idler beams of approximately 1000 laser pulses are shown in Fig. 9(a)–(c), respectively. The values of the pointing stability were calculated from standard deviation of the position of the centroids from the mean values and listed in Table 2. The fluctuation of the peak intensity from pulse to pulse of the Ho:YAG, signal and idler beam measured at a distance of 1.5 m from the output coupler is shown in Fig. 10. The fluctuation of the peak intensity of the Ho:YAG beam is in the range of ±4% and ±12% and ±8% of the signal and idler beam, respectively. The same measurement was done after a propagation length of approximately 100 m for the signal and idler beam. The results are shown in Fig. 11. The fluctuation of the peak intensity of the idler beam was significantly higher in the range of ±22%, whereas the fluctuation of the signal beam remained nearly unchanged (±13%). This effect could be explained by the partial overlap of the idler spectrum (spectral width ∼250 nm) with the CO_2 absorption band centered at 4.25 μm and several water absorption lines at $\lambda > 4.5$ μm. The atmospheric transmission over a length of 27 m was calculated assuming a relative humidity of 50% at 25° C and a CO_2 concentration of 360 ppm. This results in 100% transmission for the signal and 92% transmission for the idler spectrum centered at 3.9 μm and 4.5 μm, respectively. With a power meter losses of ∼3% of the signal and ∼8% of the idler beam were measured over a length of 27 m.

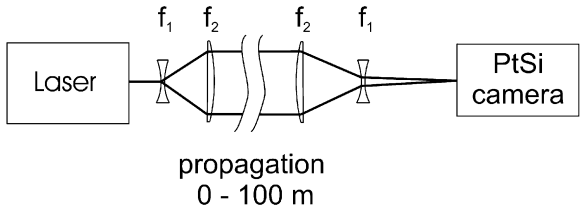

Fig. 8. Experimental setup to measure the pointing stability and for the propagation experiments of the Ho:YAG and ZGP OPO beams.

Table 2
Results of pointing stability measurements

	$\delta\alpha_x$ (μrad)	$\delta\alpha_y$ (μrad)
Ho:YAG ($\lambda = 2.09$ μm)	14	18
ZGP signal ($\lambda = 3.9$ μm)	26	22
ZGP idler ($\lambda = 4.5$ μm)	19	20

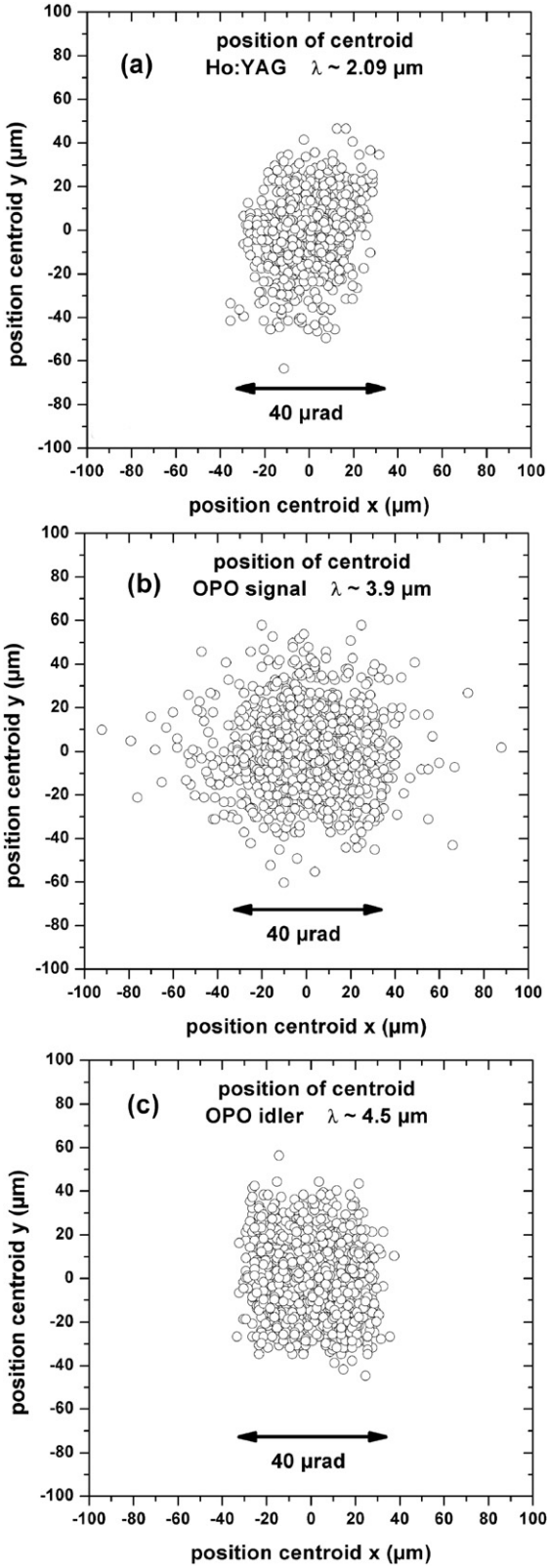

Fig. 9. Positions of centroid of approximately 1000 pulses of (a) Ho:YAG, (b) signal and (c) idler beam.

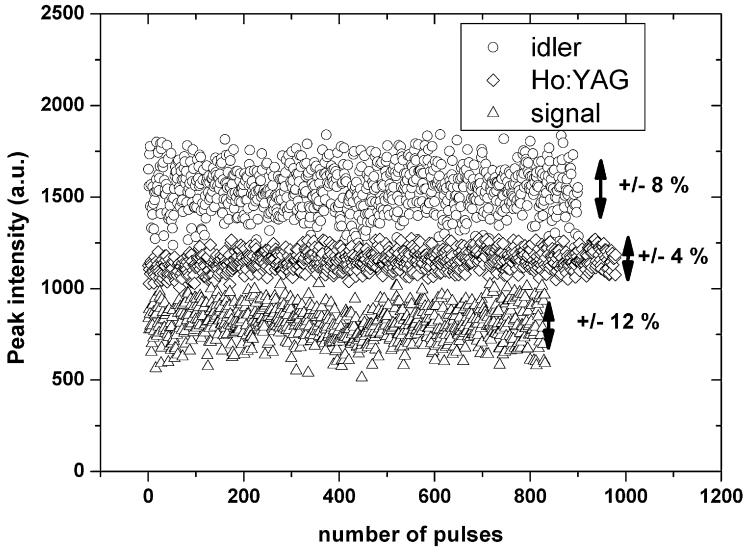

Fig. 10. Fluctuation of peak intensity from pulse to pulse of Ho:YAG, signal and idler beam measured at a distance of 1.5 m from the output coupler.

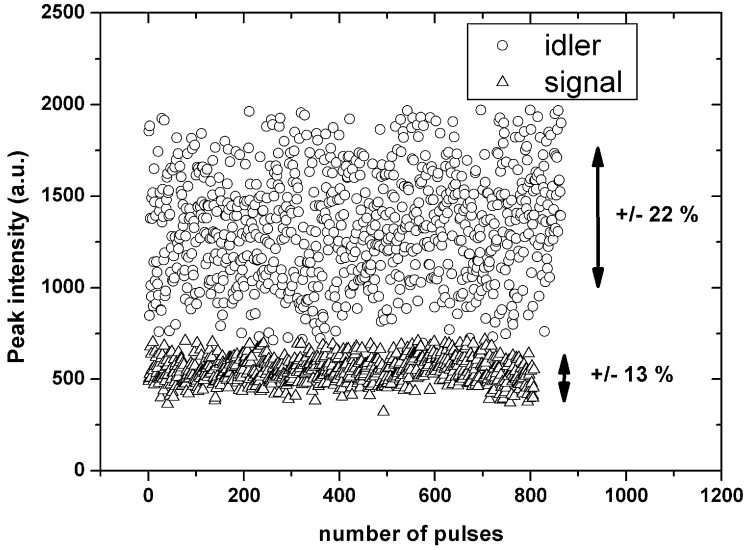

Fig. 11. Fluctuation of peak intensity from pulse to pulse of signal and idler beam measured at a distance of 100 m from the output coupler.

5. Conclusions

An efficient system for the generation of tunable, multiwatt midinfrared laser radiation has been implemented. Two polarization coupled diode-pumped Tm:YLF lasers were used to pump a Q-switched Ho:YAG laser. 21 W of average power at repetition rates of 10–50 kHz was obtained with $M^2 < 2$. This radiation was converted to the 3–5 μm range in a ZGP-based OPO, that has been designed as a double-pass doubly resonant (DPDRO) OPO. A total output power in the 3–5 μm band of 10.6 W at 10 kHz and 8.5 W at 20 kHz was obtained. Optical-to-optical efficiency achieved is >8.8% (laser-diode 792 nm to mid-IR 3–5 μm). With a commercial PtSi infrared camera (256 × 256 pixel focal plane array, 24 μm pitch) the pointing stability of Ho pump, signal and idler beam was measured to be better than 30 μrad. Propagating the OPO beams over ∼100 m, little absorption for the idler beam was observed, resulting in a significant higher peak-to-peak value of ±22%, whereas the peak-to-peak stability of the signal pulses remained unchanged (±13%).

Acknowledgement

This work was supported by the Bundesamt für Wehrtechnik und Beschaffung, under contract BWB E/T 43 X/5 A 108/6 F 860 [10].

References

[1] P.A. Budni, M.L. Lemons, J.R. Mosto, E.P. Chicklis, IEEE J. Selected Topics in Quantum Electr. 6 (2000) 629.
[2] E. Lippert, S. Nicolas, G. Arisholm, K. Stenersen, G. Rustad, Appl. Opt. 45 (2006) 3839.
[3] C. Bollig, R.A. Hayward, W.A. Clarkson, D.C. Hanna, Opt. Lett. 23 (1998) 1757.
[4] M. Schellhorn, A. Hirth, C. Kieleck, Opt. Lett. 28 (2003) 1933.
[5] D.Y. Shen, A. Abdolvand, L.J. Cooper, W.A. Clarkson, Appl. Phys. B 79 (2004) 559.
[6] P.A. Budni, L.A. Pomeranz, M.L. Lemons, C.A. Miller, J.R. Mosto, E.P. Chicklis, J. Opt. Soc. Am. B 17 (2000) 723.
[7] G. Arisholm, E. Lippert, G. Rustad, K. Stenersen, Opt. Lett. 25 (2000) 1654.
[8] Charakterisierung von Laserstrahlen und Laseroptiken: Normen, DIN – Taschenbuch, vol. 341, DIN, Deutsches Institut für Normung e.V., ISBN 3-410-15063-3, 2001.